9. D. S. Olton, J. T. Becker, G. E. Handelmann, *Behav. Brain Sci.* **2**, 313 (1979); C. A. Barnes, *Trends Neurosci.* **11**, 163 (1988); R. J. Sutherland and J. W. Rudy, *Psychobiology* **17**, 129 (1989).
10. L. R. Squire, *Memory and Brain* (Oxford Univ. Press, New York, 1987). Memory for facts and events (declarative memory) can be contrasted with skill-learning, priming, conditioning, and other forms of nondeclarative (implicit) memory, which are independent of the hippocampal formation.
11. T. Ribot, *Les Maladies de la Memoire* (Germer Baillere, Paris, 1881) [English translation: *Diseases of Memory* (Appleton-Century-Crofts, New York, 1882)]. The phenomenon of temporally graded retrograde amnesia has been confirmed repeatedly in rodents with a variety of memory tasks and disruptive treatments [J. L. McGaugh and P. E. Gold, in *Neural Mechanisms of Learning and Memory*, M. Rosenzweig and E. Bennett, Eds. (MIT Press, Cambridge, MA, 1976), pp. 549–560].
12. D. MacKinnon and L. R. Squire, *Psychobiology* **17**, 247 (1989).
13. L. R. Squire, F. Haist, A. P. Shimamura, *J. Neurosci.* **9**, 828 (1989).
14. With most tests available for assessing remote memory in humans, one cannot be sure that past time periods are being sampled equivalently [L. R. Squire, *Neuropsychologia* **12**, 429 (1974)]. Accordingly, for any time period it is difficult to know whether the score on a remote memory test reflects the age of the memories or the difficulty of the questions. Also see E. E. Coons and N. E. Miller, *J. Comp. Physiol. Psychol.* **53**, 524 (1960).
15. The H^+ lesion included the hippocampus proper, the dentate gyrus, the subicular complex, the posterior entorhinal cortex, and most of the parahippocampal cortex (7).
16. Testing was carried out in a Wisconsin General Test Apparatus [H. Harlow and J. A. Bromer, *Psychol. Rec.* **19**, 434 (1938)]. For each object pair, a raisin reward was concealed under the correct object. Assignment of the five sets of training objects to the five preoperative training periods was balanced across monkeys. The 20 object pairs in each set were always presented in the same order to each monkey.
17. The five preoperative training episodes began for all monkeys exactly 109, 81, 53, 25, and 11 days before surgery and were completed 10 days later. To measure how well the object pairs were learned preoperatively, an additional test was administered 1 day after training was completed on each 20-pair set. For these tests, all 20 object pairs were presented once to each monkey in the same random order during a single session.
18. The learning scores for the five training episodes were 70.0, 73.9, 77.1, 75.8, and 75.8% correct (from the first to the last episode, respectively, and averaging across 14 training trials, 20 object pairs, and 18 monkeys). A two-way analysis of variance (learning trials × training episodes) showed marked learning within each episode [$F(6,24) = 177$, $P < 0.001$], a numerically small but significant effect of training episode [$F(4,24) = 17.4$, $P < 0.001$], and no interaction. For this analysis, the 14 learning trials were blocked into seven groups of two trials each. The scores for the monkeys who were later given hippocampal lesions were virtually identical to the scores of the monkeys who served as unoperated controls (within 2.5% for each training episode).
19. At the 12-week time period, the data for normal monkeys were quite variable (standard error = 5.3%), and the comparison between normal and operated monkeys was not significant ($P = 0.12$).
20. The issue of interest is whether the memory scores of operated monkeys increase significantly as one moves from a recent to a more remote time period, not whether such an increase extends to every remote time period in the study. Indeed, in very remote time periods the scores of operated monkeys would be expected to join the forgetting curve of normal monkeys.
21. Assume that some acquired information will be remembered for a long time and that other information will be remembered for a relatively short time. Both kinds of information must be more abundant shortly after learning than at later times. If hippocampal damage affects information that is ordinarily short-lived, then what survives in memory after damage will be relatively long-lasting information, and it will be at least as abundant in recent time periods as in more remote time periods. Accordingly, after hippocampal damage, performance scores should always be at least as good for the most recent time period (that is, for the period just before the time of damage), as for any more remote time period. The limiting case would have performance scores equal across all time periods. The present finding, that retention was significantly poorer for recent time periods than for more remote time periods, rules out this account of temporally graded retrograde amnesia.
22. For earlier versions of the consolidation concept, see G. E. Muller and A. Pilzecker, *Z. Psychol.* **1**, 1 (1900); J. L. McGaugh and M. Herz, *Memory Consolidation* (Albion, San Francisco, 1972); S. E. Glickman, *Psychol. Bull.* **58**, 218 (1961); L. R. Squire, *Annu. Rev. Neurosci.* **5**, 241 (1982).
23. Gradients of retrograde amnesia have been obtained previously, in which the remote past was remembered better than the recent past: with psychiatric patients prescribed electroconvulsive therapy [L. R. Squire, P. C. Slater, P. M. Chace, *Science* **187**, 77 (1975)] and in prospective tests of mice given electroconvulsive shock [L. R. Squire and C. W. Spanis, *Behav. Neurosci.* **98**, 345 (1984)]. However, results with convulsive stimulation cannot be directly related to neuroanatomy or to hippocampal function. Recently, this same kind of temporal gradient of retrograde amnesia was described in rats after hippocampal lesions; in this case, the gradient extended 2 to 5 days [G. Winocur, *Behav. Brain Res.* **38**, 145 (1990); also see R. Sutherland *et al.*, *Soc. Neurosci. Abst.* **13**, 1066 (1987)]. In monkeys with more extensive medial temporal lobe lesions and overtraining of object pairs, temporally graded retrograde amnesia was not observed [D. Salmon, S. Zola-Morgan, L. R. Squire, *Psychobiology* **15**, 37 (1987)].
24. D. Marr, *Philos. Trans. R. Soc. London Ser. B* **176**, 23 (1971); B. McNaughton, in *Neural Connections, Mental Computations*, L. Nadel, L. A. Cooper, P. Culicover, R. M. Harnish, Eds. (MIT Press, Cambridge, MA, 1989), pp. 285–350; E. Rolls, in *An Introduction to Neural and Electronic Networks*, S. F. Zornetzer, J. L. Davis, C. Lau, Eds. (Academic Press, San Diego, CA, 1990), pp. 73–90; T. J. Tyler and P. Discenna, *Behav. Neurosci.* **100**, 147 (1986); P. Milner, *Neuropsychologia* **27**, 23 (1989); E. Halgren, in *Neuropsychology of Memory*, L. R. Squire and N. Butters, Eds. (Guilford, New York, 1984), pp. 165–182; L. R. Squire, N. Cohen, L. Nadel, in *Memory Consolidation*, H. Weingartner, E. Parks, Eds. (Erlbaum, Hillsdale, NJ, 1984), pp. 185–210; L. R. Squire, A. Shimamura, D. G. Amaral, in *Neural Models of Plasticity*, J. Byrne and W. Berry, Eds. (Academic Press, New York, 1989), pp. 208–239.
25. M. Mishkin, *Philos. Trans. R. Soc. London Ser. B* **298**, 85 (1982); A. R. Damasio, *Cognition* **33**, 25 (1989).
26. We thank C. LeClair, R. Clower, and D. Amaral for assistance. Supported by the Medical Research Service of the Department of Veterans Affairs, the Office of Naval Research, NIH grant NS19063, National Institute of Mental Health grant MH24600, the McKnight Foundation, and a bioscience grant for International Joint Research from the New Energy and Industrial Technology Development Organization, Japan.

7 June 1990; accepted 27 August 1990

Widespread Expression of BDNF But Not NT3 by Target Areas of Basal Forebrain Cholinergic Neurons

HEIDI S. PHILLIPS,* JEANNE M. HAINS, GARY R. LARAMEE, ARNON ROSENTHAL, JOHN W. WINSLOW

Brain-derived neurotrophic factor (BDNF) and neurotrophin-3 (NT3) are homologs of the well-known neurotrophic factor nerve growth factor. The three members of this family display distinct patterns of target specificity. To examine the distribution in brain of messenger RNA for these molecules, in situ hybridization was performed. Cells hybridizing intensely to antisense BDNF probe were located throughout the major targets of the rat basal forebrain cholinergic system, that is, the hippocampus, amygdala, and neocortex. Strongly hybridizing cells were also observed in structures associated with the olfactory system. The distribution of NT3 mRNA in forebrain was much more limited. Within the hippocampus, labeled cells were restricted to CA2, the most medial portion of CA1, and the dentate gyrus. In human hippocampus, cells expressing BDNF mRNA are distributed in a fashion similar to that observed in the rat. These findings point to both basal forebrain cholinergic cells and olfactory pathways as potential central targets for BDNF.

THE PROTOTYPIC NEUROTROPHIC fac-tor nerve growth factor (NGF) has recently gained much attention as a potential therapeutic agent for Alzheimer's disease by virtue of its apparent trophic action on cholinergic forebrain neurons (*1*). Although the more recently described neurotrophic factors BDNF and NT3 are present in the central nervous system (*2–4*), little is known about the sources or targets for these molecules in the brain. To localize mRNA for BDNF and NT3 in rat brain, we performed in situ hybridization at high stringency (*5*) with ^{35}S-labeled RNA probes (*6*). An initial survey of the brain revealed a striking pattern of BDNF hybridization in several forebrain regions. Significant labeling for BDNF mRNA was also observed in

Department of Developmental Biology, Genentech, South San Francisco, CA 94080.

*To whom correspondence should be addressed.

the midbrain, pons, and medulla, but as individual cells were less intensely labeled, we focused on examination of coronal sections through the forebrain (7).

Within the forebrain, we saw cells hybridizing strongly for BDNF with the antisense probe in the neocortex, basolateral amygdala, hippocampus, and projection areas of the main olfactory system (Fig. 1, A, C, and E). Control sections that hybridized with the sense-strand probe showed only a few evenly distributed silver grains (Fig. 1, B, D, and F, and Fig. 2B). In the hippocampal formation, both the pyramidal layer of CA1 to CA4 and the dentate gyrus were labeled by the antisense probe (Fig. 1, C and E, and Fig. 2G). A distinct subpopulation of cells in the pyramidal layer was apparent by virtue of its relatively intense reaction with the BDNF probe (Fig. 2, E and F). The granule cell layer of the dentate gyrus was more uniformly labeled. Numerous regions of the neocortex showed hybridization to the antisense BDNF probe; the anterior cingulate and perirhinal areas displayed particularly prominent signals (Fig. 1, A, C, and E, and Fig. 2, A, C, and D). Although positive cells could be seen in layers 2 through 6 of the neocortex, layers 2, 3, and 6 contained the greatest concentrations of such cells.

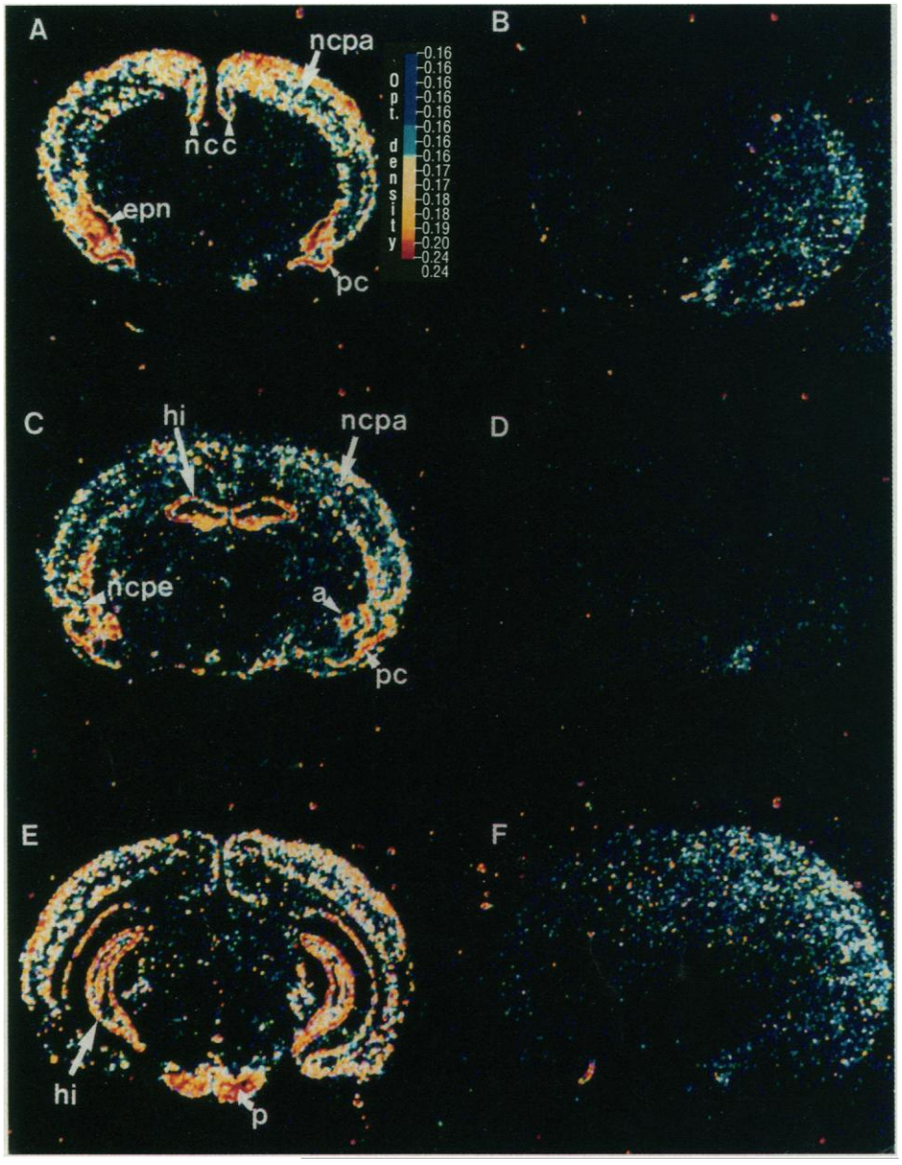

Fig. 1. Computer-enhanced images of in situ hybridization for BDNF at three forebrain levels. (**A**, **C**, and **E**) Images of sections hybridized with antisense probe. (**B**, **D**, and **F**) Images of corresponding sections hybridized with sense strand control probe. All images displayed depict sheet film autoradiographs digitized and enhanced under identical conditions. The color scale in (A) applies to all other panels. Sections in (A), (C), and (E) correspond to the coordinates +1.0 mm, −2.3 mm, and −6.2 mm, respectively, anterior to bregma according to (*14*). a, amygdala; epn, endopyriform nucleus; hi, hippocampus; ncc, neocortex, cingulate region; ncpa, neocortex, parietal area; ncpe, neocortex, perirhinal region; p, pons; pc, pyriform cortex. Unfixed brains from male Sprague-Dawley rats (1 to 3 months of age) killed by carbon dioxide–induced asphyxia were cryosectioned at a thickness of 12 μm and hybridized under high stringency conditions (*5*).

Strong hybridization was also seen in numerous olfactory regions. Cells labeled with the BDNF probe were apparent in several targets of the lateral olfactory tract, including the anterior olfactory nucleus (not shown), cortical nucleus of the amygdala (not shown), layer 2 pyriform cortex (Fig. 1A), entorhinal cortex (Fig. 1E), and tenia tecta (Fig. 2A). The endopyriform nucleus was also prominently labeled (Fig. 1A). The olfactory bulb proper did not contain strongly hybridizing cells.

The pattern of brain localization of BDNF mRNA significantly overlaps the distribution of NGF mRNA previously observed (*8*). Cells hybridizing strongly for BDNF mRNA were observed in all regions that contain cells with detectable mRNA for NGF. In order to determine whether all members of the NGF family of trophic molecules exhibit a similar pattern of expression in brain, we compared hybridizations with probes to the three known members of this family: NGF, BDNF, and NT3. We evaluated the specificity of our probes to BDNF and NT3 by comparing hybridization of these probes to mouse salivary gland and brain with hybridization of an NGF probe to the same tissues. Our BDNF and NT3 probes did not cross-hybridize with NGF mRNA since they did not react with salivary gland under conditions that allowed intense hybridization with the NGF probe (Fig. 3, A to D) (*9*).

In brain, the probes to NGF, BDNF, and NT3 each produced a distinct pattern of hybridization (Fig. 3, E through H) (*10*). In contrast to BDNF, which was consistently expressed throughout the target areas of basal forebrain cholinergic neurons (Fig. 3E), NT3 expression was limited (Fig. 3G). No significant hybridization for NT3 was seen in cingulate, temporal, or parietal regions of the neocortex, in the amygdala, or within endopyriform nucleus. Weak to moderate labeling was observed in layer 2 of the pyriform cortex (Fig. 3G), and scattered labeled cells were apparent in posterior neocortical regions (not shown). We found the strongest signal for NT3 within the hippocampus. Unlike BDNF hybridization, which was evident throughout the hippocampus and dentate gyrus (Figs. 2G and 3E), NT3 labeling was restricted to the dentate gyrus, CA2, and the most medial region of CA1 (Figs. 2H and 3G). Regions hybridizing to the NGF probe showed ex-

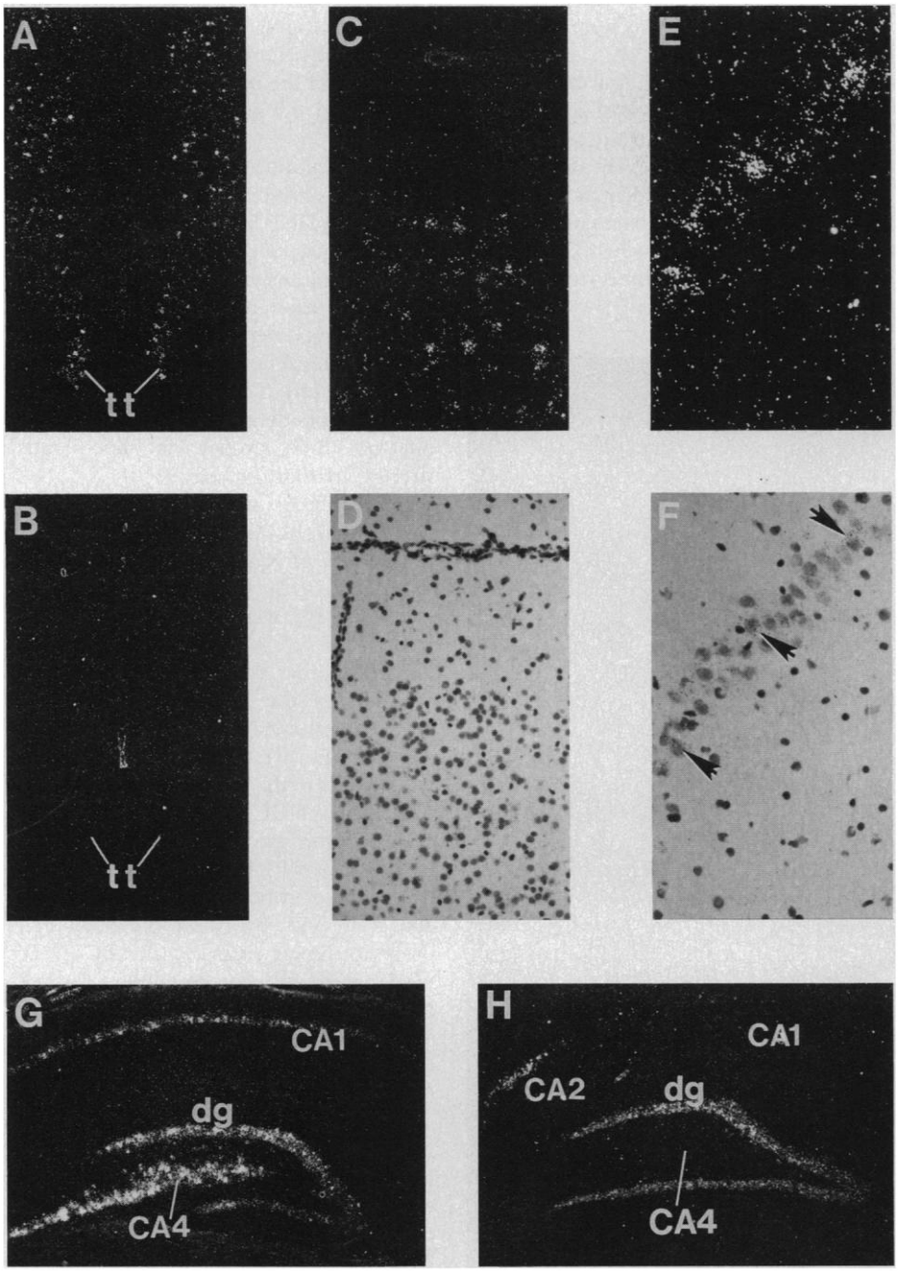

Fig. 2. Emulsion autoradiographs of rat brain. (A) through (G) are coronal sections hybridized to sense or antisense BDNF probes as described in the legend to Fig. 1. (H) is a sagittal section hybridized to NT3 antisense probe. (A through F and H) are 12-μm sections of brain that were not fixed before sectioning, and (G) is a 40-μm section of a brain fixed in 4% paraformaldehyde by intracardiac perfusion and cryoprotected in 15% sucrose. (**A** and **B**) Adjacent sections through the tenia tecta (tt) and cingulate cortex (upper two thirds of micrograph) probed with antisense (A) and sense (B) probes. Numerous cells in the tenia tecta and layers 2 and 3 of the cingulate cortex hybridize specifically to the antisense probe. Refractive object in the center of (B) is a blood vessel that does not show a significant accumulation of silver grains. (**C** and **D**) Dark-field and bright-field views of the superficial layers of the anterior cingulate cortex from a section hybridized with antisense probe. Several labeled cells are visible in layers 2 and 3 (lower half of micrograph). Layer 1 is devoid of labeled cells (upper half). The pial surface is visible in the upper portion of (D). (**E** and **F**) Dark-field and bright-field views of a section through the pyramidal layer of hippocampus (CA2 and CA3) hybridized with antisense probe. A distinct subpopulation of cells in the pyramidal layer [arrows in (F)] is labeled intensely. The large round nuclei of the reactive cells are similar in appearance to those of pyramidal cells. (**G**) Section through hippocampal formation hybridized with antisense probe to BDNF. Labeled cells are visible in the dentate gyrus (dg), and all subdivisions of Ammon's horn (CA1 and CA4 are indicated). (**H**) Section through hippocampal formation hybridized with antisense NT3 probe. Labeling is visible only in CA2 and dentate gyrus. Magnifications: (A and B) ×70; (C and D) ×275; (E and F) ×400; (G and H) ×85.

tensive overlap with those reactive for BDNF mRNA. The distribution of NGF mRNA differed somewhat between rat and mouse brain. In both species, however, we saw significant differences in the hybridization patterns of NGF and BDNF. For instance, in mouse brain, the BDNF hybridization signal was markedly higher than that of NGF in cortex and dentate gyrus, and markedly lower than the NGF signal in several thalamic nuclei (Fig. 3, E and F).

Our observations indicate that the widespread expression of BDNF by cortex, hippocampus, amygdala, and the olfactory system is not a general feature of all NGF homologs. As the neocortex, hippocampus, and amygdala are among the main targets of the basal forebrain cholinergic system, the expression of BDNF within these regions suggests that BDNF might act as a trophic factor for this system. The more restricted distribution of NT3 within hippocampus and its paucity within cortex argues that this factor is less likely to serve a major role in the maintenance of large numbers of basal forebrain cholinergic neurons. In fact, studies performed in parallel to these (*11*) indicate that BDNF but not NT3 can enhance the cholinergic properties of cultures of embryonic basal forebrain. The demonstration that BDNF is expressed in targets of both the olfactory system and the basal forebrain cholinergic system is intriguing in light of the critical involvement of these systems in Alzheimer's disease (*12*).

In order to extend our findings on BDNF expression, sections through hippocampus of human postmortem tissue were subjected to hybridization with an antisense RNA probe for the human BDNF mRNA sequence (*13*). Although the strength of the hybridization signal varied in the samples of tissue examined, a positive signal was seen throughout the dentate gyrus and Ammon's horn in most cases (Fig. 4). The results were similar to our observations in rat: the granule layer of the dentate gyrus was uniformly labeled, whereas a subpopulation of cells in the pyramidal layer of CA1 to CA4 displayed dense accumulations of silver grains (not shown). These observations indicate that BDNF is expressed in the adult human brain by one of the major targets of the basal forebrain cholinergic neurons.

REFERENCES AND NOTES

1. For reviews, see J. Marx, *Science* **247**, 408 (1990); F. Hefti, J. Hartikka, B. Knusel, *Neurobiol. Aging* **10**, 515 (1989); *Science* **243**, 11 (1989).
2. Y.-A. Barde *et al.*, *EMBO J.* **1**, 549 (1982); A. M. Davies, *Trends Neurosci.* **11**, 243 (1988); Y.-A. Barde, *Neuron* **2**, 1525 (1989); A. Hohn, J. Leibrock, K. Bailey, Y.-A. Barde, *Nature* **34**, 339 (1990); J. Leibrock *et al.*, *ibid.* **341**, 149 (1989).
3. P. C. Maisonpierre *et al.*, *Science* **247**, 1446 (1990).

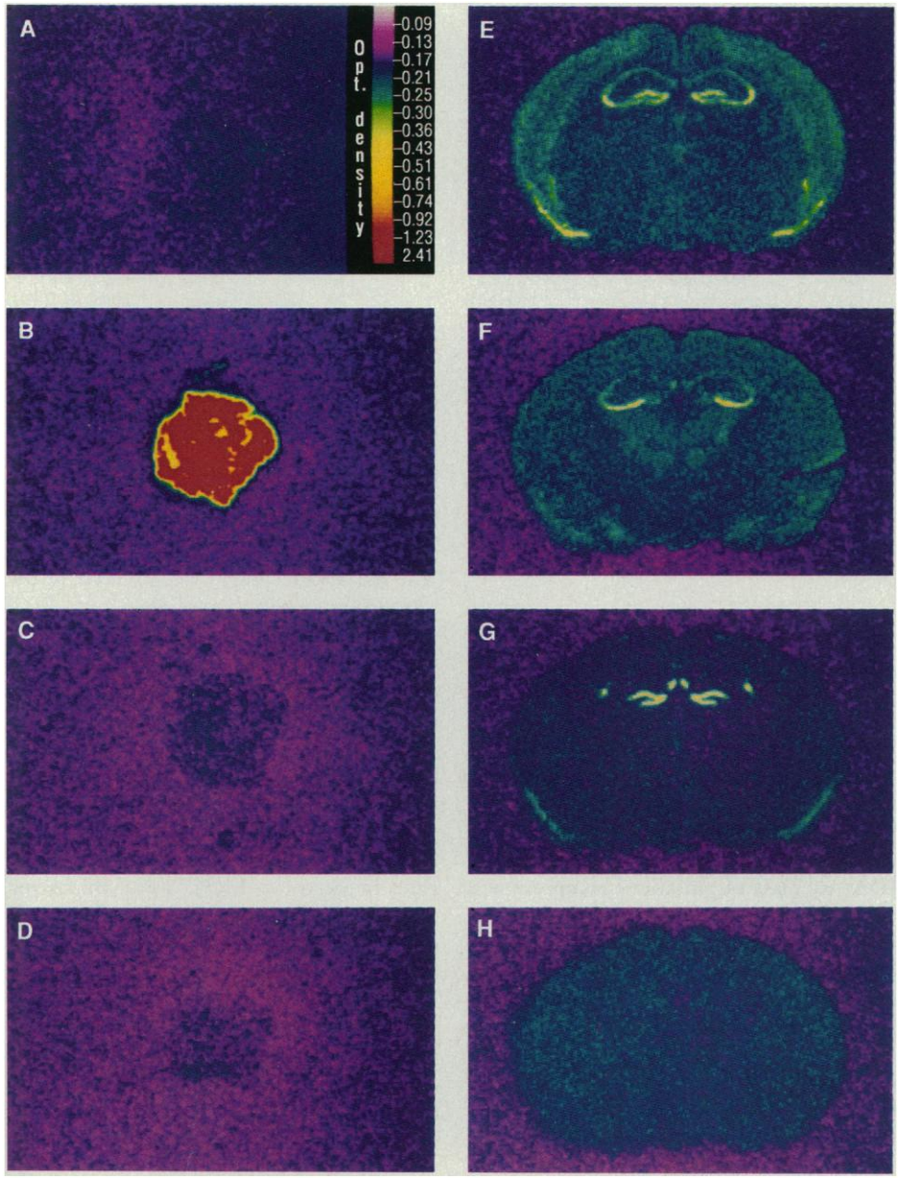

Fig. 3. Computer-digitized film autoradiographs of male mouse salivary gland (A through D) and brain (E through H). (**A** and **E**) BDNF antisense probe. (**B** and **F**) NGF antisense probe. (**C** and **G**) NT3 antisense and (**D** and **H**) BDNF sense probes. Probe synthesis and hybridizations were carried out as described (*5, 6*). The NGF probe was generated with a 963-bp fragment of mouse NGF (Sma I to Pst I, 66 to 1029) cloned into pSP64 as template (*15*). Exposure times: 30 hours (A through D), 5 days (E through H). Color scale applies to all panels.

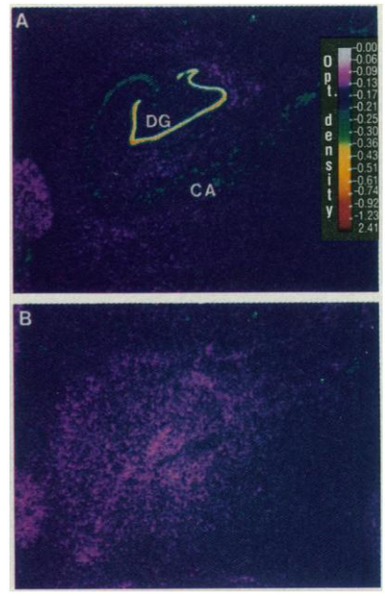

Fig. 4. Computer-digitized autoradiographs of human hippocampus hybridized to BDNF antisense (A) and sense (B) probes. A strong hybridization signal is observed in the granule layer of the dentate gyrus (DG). On emulsion autoradiographs, this signal is evenly distributed over all of the cells in this layer (not shown). Significant hybridization signal is also associated with the pyramidal layer of CA1 to CA4. Emulsion images reveal that a subpopulation of cells within the pyramidal layer is intensely reactive.

4. A. Rosenthal *et al.*, *Neuron* **4**, 767 (1990).
5. Hybridizations were carried out by a modification of the method of Wilcox *et al.* [*J. Clin. Invest.* **82**, 1134 (1988)]. Before hybridization, tissue sections of fresh frozen brain were fixed for 30 min in 4% formaldehyde at 4°C (with or without 1% glutaraldehyde), rinsed in 0.5× SSC (20× SSC is 3 M NaCl and 0.3 M sodium citrate), and incubated with hybridization buffer (400 μl per slide) without probe at 42°C for 1 hour. Hybridization buffer consisted of 50% formamide, 0.1 M NaCl, 20 mM tris (pH 8.0), 5 mM EDTA, 1× Denhardt's solution, 10% dextran sulfate, and 10 mM dithiothreitol. Probes were added in a small volume of buffer to a final concentration of 8×10^6 cpm/ml, and hybridization was carried out at 55°C overnight. A series of rinses in 2× SSC containing 10 mM β-mercaptoethanol (β-ME) and EDTA (1 mM) preceded and followed a 30-min treatment at room temperature with ribonuclease (RNase) (20 μg/ml in 0.5 M NaCl and 10 mM tris, pH 8.0). A stringency wash was then carried out in a large volume of 0.1× SSC containing β-ME (10 mM) and EDTA (1 mM) at 55°C for 2 hours. Sections were washed in 0.5× SSC, dehydrated in ethanol containing ammonium acetate (0.3 M), dried under low vacuum, and exposed to sheet film (Hyperfilm-β max, Amersham) or NTB2 emulsion. (Kodak).
6. ^{35}S-labeled RNA probes were generated as described [D. A. Melton *et al.*, *Nucleic Acids Res.* **12**, 7035 (1984)]. Sense and antisense probes were made with the use of T7 and SP6 polymerases, respectively. Probes for BDNF were generated with a 460-bp template of rat BDNF subcloned into pGEM-4Z (Promega). The cDNA template was derived from a clone of a rat forebrain λgt10 cDNA library. The clone was identified by screening the library with a 186-bp oligonucleotide (generated by polymerase chain reaction) corresponding to residues 762 to 948 of human BDNF (A. Rosenthal *et al.*, in preparation). The 460-bp cDNA fragment displays 90% homology with both human and porcine sequences (*3*). The 5′ end matches residue 756 of the published porcine sequence. For NT3, a 473-bp probe corresponding to residues 375 to 848 of the rat sequence (*4*) was utilized for hybridizations, which were carried out as described (*5*) with brains from male rats 4 to 5 weeks of age.
7. One complete series of coronal sections of unfixed brain through the forebrain was examined. Sets of four consecutive sections (12 μm thickness) were cut at intervals of 288 μm. Two sections of each set were utilized for hybridization with antisense probe and two with sense probe. Areas revealing a significant degree of hybridization were examined in at least two additional experiments with tissue from separate animals.
8. D. Shelton and L. Reichardt, *Proc. Natl. Acad. Sci. U.S.A.* **83**, 2714 (1986); C. Ayer-LeLievre, L. Olson, T. Ebendahl, A. Seiger, H. Persson, *Science* **240**, 1339 (1988); C. M. Gall and P. J. Isackson, *ibid.* **245**, 758 (1989).
9. The specificity of BDNF and NT3 probes was further verified on Northern blots of tissue RNA, slot blots of RNA generated by in vitro transcription, and by in situ hybridizations in the presence of competing sense strand RNAs. In one experiment, we demonstrated the specificity of the NT3 probe by observing that the signal in hippocampus (probe concentration of ~0.045 nM) could be eliminated by competition with sense strand RNA for NT3 (0.06 to 1 nM), but not NGF or BDNF. A similar experiment was not performed for the BDNF probe, because of the lack of an NGF clone containing sufficient 3′ untranslated sequence to correspond to the entire length of our BDNF probe. The specificity of the BDNF probe was verified by its failure to recognize NT3 or NGF RNA (generated by in vitro transcription) on slot blots hybridized under conditions virtually identical to our in situ hybridization procedure. Northern analysis of polyadenylated RNA isolated from ten rat tissues was performed with our 460-bp rat BDNF probe and a 1026-bp

NT3 probe that included the entire region utilized as a probe for in situ hybridization. The differences we observed in both the pattern of tissue distribution and transcript size (BDNF, 3.5 and 1.6 kb; NT3, 1.4 kb) are consistent with a lack of cross-hybridization of the probes among members of the NGF family.
10. The localization of mRNA for BDNF, NT3, and NGF was compared in coronal sections of rat and mouse forebrain. The distribution of BDNF, NT3, and NGF mRNA in sections of rat and mouse brain through the hippocampus was examined in four separate experiments with tissue from 12 rats and 7 mice.
11. B. Knüsel *et al.*, in preparation.
12. B. R. Talamo *et al.*, *Nature* **337**, 736 (1989); P. F. Reyes *et al.*, *Arch. Neurol.* **44**, 644 (1987); J. A. Hardy, *et al.*, *Neurobiol. Aging*, 7, 489 (1986); R. Pearson *et al.*, *Proc. Natl. Acad. Sci. U.S.A.* **82**, 4531 (1985); P. J. Whitehouse, D. L. Price, A. E. Clark, J. T. Coyle, M. R. DeLong, *Ann. Neurol.* **10**, 122 (1981).
13. Hybridizations were carried out as described (*5*). Templates for the sense and antisense probes were derived from a cDNA clone encoding for human BDNF (A. Rosenthal *et al.*, in preparation). The template and resulting probes were approximately 1 kb and contained ~600 bp of protein coding sequence and ~300 bp of 3′ untranslated sequence. On slot blots, this probe gave no detectable hybridization to RNA encoding for human NGF or NT3 at concentrations of these RNAs in 20-fold excess over that required for a hybridization signal to BDNF.
14. G. Cain and C. Paxinos, *The Rat Brain in Stereotaxic Coordinates* (Academic Press, San Diego, CA, 1986).
15. J. Scott *et al.*, *Nature* **302**, 538 (1983).
16. We thank K. Nikolics for support and encouragement, J. Wilcox for sharing in situ hybridization protocol, M. Armanini for technical assistance, and T. Altar for the use of the image analysis system. The clone encoding for mouse NGF was provided by L. Reichardt. Human tissue specimens were obtained from the National Neurological Research Bank, VAMC Wadsworth Division, Los Angeles, CA 90073, which is sponsored by NINDS, NIH/NIMH, National Multiple Sclerosis Society, Huntington's Disease Foundation, Comprehensive Epilepsy Program, Tourette Syndrome Association, Dystonia Medical Research Foundation, and Veterans Health Services and Research Administration, Department of Veterans Affairs. We thank W. W. Tourtellotte, D. Matoff, and J. Riehl for their assistance in providing these specimens.

25 April 1990; accepted 23 August 1990

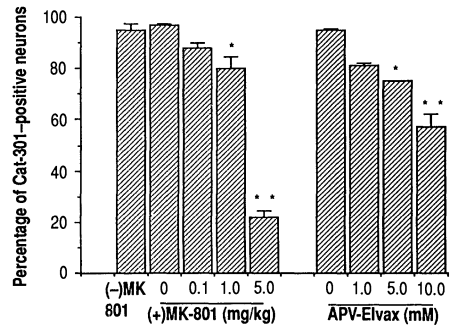

Fig. 1. MK-801 and APV inhibit Cat-301 immunoreactivity on sciatic motor neurons. Sample preparation as in Table 1. Scheffé's multiple-range test for comparisons within several experimental groups was used to show differences from vehicle-treated animals (*, $P < 0.05$; **, $P < 0.01$). The percentage of Cat-301–positive neurons from (–)MK-801–treated animals did not differ significantly from that of saline-injected controls.

Induction of a Neuronal Proteoglycan by the NMDA Receptor in the Developing Spinal Cord

ROBERT G. KALB* AND SUSAN HOCKFIELD

Activation of the *N*-methyl-D-aspartate (NMDA) subclass of glutamate receptors is a critical step in the selection of appropriate synaptic connections in the developing visual systems of cat and frog. Activity-dependent development of mammalian motor neurons was shown to be similarly mediated by activation of the NMDA receptor. The expression of the Cat-301 proteoglycan on motor neurons was developmentally regulated and could be specifically inhibited by blockade of the NMDA receptor at the spinal segmental level. In the adult, Cat-301 immunoreactivity on motor neurons was not diminished by NMDA receptor blockade. The NMDA receptor may regulate the expression of a class of neuronal proteins (of which Cat-301 is one example) that underlie the morphological and physiological features of activity-dependent development.

NEURONAL ACTIVITY IN THE EARLY postnatal period can have long-lasting effects on both the anatomy and physiology of neurons in the mammalian central nervous system (CNS). In many systems, activity-dependent effects on neuronal phenotype occur during circumscribed periods in early postnatal development, called critical or sensitive periods (*1*). In the cat visual cortex, activity-dependent acquisition of mature neuronal properties has been suggested to involve activation of the NMDA subclass of glutamate receptors (*2*). The molecular events that follow activation of the NMDA receptor and lead to alterations in neuronal phenotype are only beginning to be understood, but one hypothesis suggests that NMDA receptor activation leads to changes in the expression of neuronal proteins.

The expression of the neuronal cell surface proteoglycan recognized by monoclonal antibody Cat-301 (*3*) is regulated by neuronal activity in the early postnatal period. Visual deprivation of neonatal cats leads to a marked diminution of Cat-301 expression in the deprived layers of the dorsal lateral geniculate nucleus and in the visual cortex, whereas deprivation in adult cats has no effect on Cat-301 expression (*4*). Similarly, deprivation of normal patterns of neuromuscular activity in neonatal hamsters leads to a marked reduction in the expression of the Cat-301 proteoglycan on spinal cord motor neurons, whereas deprivation in adults does not (*5, 6*). The perisynaptic location (*7*) and developmental regulation (*4–6*) of the Cat-301 proteoglycan suggest that the antigen might be involved in the selection or stabilization of the mature set of synapses on motor neurons.

The expression of the Cat-301 antigen on motor neurons requires input from several sources (segmental and suprasegmental) in early life. At birth, hamster spinal motor neurons do not express the Cat-301 antigen; adult levels of expression are reached by the end of the second postnatal week (*5*). Disrupting sciatic motor neuron activity in neonates by nerve crush (*5*), dorsal rhizotomy (*6*), or thoracic cordotomy (*5*) at postnatal day 7 (P7) (before the onset of normal Cat-301 expression) inhibits the development of Cat-301 immunoreactivity on motor neurons. When adult animals are subjected to the same lesions, no effect on Cat-301 expression is seen. These studies provide molecular evidence for activity-dependent development of motor neurons.

Large-diameter primary afferents are required for normal expression of Cat-301 (*6*), and some of these are glutamatergic (*8*). Glutamate is considered the primary excitatory neurotransmitter in the spinal cord, and polysynaptic activation of motor neurons involves activation of the NMDA receptor (*9, 10*). The established role of NMDA receptors in activity-dependent development in other systems led us to explore the possibility that the NMDA receptor might also play a role in the maturation of spinal motor neurons, as assayed by Cat-301 expression.

As a first step in evaluating the effects of NMDA receptor blockade on the expression of Cat-301 immunoreactivity, we employed the lipophilic, noncompetitive NMDA receptor antagonist, MK-801. Animals received intraperitoneal injections of MK-801 daily from P7 to P21 at a range of doses (0.1 to 5.0 mg per kilogram of body weight). At first, animals appeared intoxicated, but

Section of Neuroanatomy, Yale University School of Medicine, New Haven, CT 06510.

*To whom correspondence should be addressed.